

# Neutrinos in flat extra dimension: towards a realistic scenario

Asmaa Abada <sup>1</sup>, Paramita Dey <sup>2</sup> and Grégory Moreau <sup>3</sup>

<sup>1</sup>*Laboratoire de Physique Théorique, Université de Paris-sud XI  
Bâtiment 210, 91405 Orsay, France*

## Abstract

We consider the simple extension of the Standard Model in which an additional right handed neutrino propagates along a flat extra dimension, while the Standard Model fields are confined on a 3-brane. The fifth dimension is  $S^1/Z_2$  orbifold compactified. In this scenario, the neutrino mass can be naturally suppressed. By studying systematically the fundamental parameter space, we show that the strong phenomenological constraints on mixing angles between active and sterile neutrinos (especially those derived from the SNO experiment data) do not conflict with the possibility of generating a realistic neutrino mass spectrum. As a second step, we explore the possibility of a successful leptogenesis through the decays of the Kaluza-Klein excitations of the right handed neutrino.

PACS Nos: 11.10.Kk, 11.30.Fs, 14.60.Pq, 14.60.St, 98.80.Cq

Keywords: Extra Dimensions, Neutrino Physics

---

<sup>1</sup>E-mail address: abada@th.u-psud.fr

<sup>2</sup>E-mail address: Paramita.Dey@th.u-psud.fr

<sup>3</sup>E-mail address: moreau@th.u-psud.fr

# 1 Introduction

In the recent days, our perspectives in the search for physics beyond the Standard Model (SM) have enriched considerably with the developments of theories with extra (compact) dimensions [1–3]. In particular, these extra spatial dimensions allow to lower the gravity scale down to the TeV [1, 2], thus addressing the long standing puzzle of the gauge hierarchy problem, when gravitational interactions feel these dimensions. Such TeV-scale Extra Dimensional (ED) models have attracted a great attention from the experimentalist community, since one can undertake their precision studies in the next generation colliders. Depending on the geometry of the extra dimensions (shape and/or size), and the field localization, a wide variety of extra dimensional models have been proposed. In addition to the gauge hierarchy problem, these models address several other questions in the different avenues of particle physics, cosmology and string theory.

Among a large number of possible realizations of the ED models, the scenario, with additional right handed neutrinos (being gauge singlet, and thus sterile) in flat compact extra dimensions and SM fields localized on the brane, may provide an interesting alternative capable of accounting for the observed light neutrino masses [4–7]. Also, the detailed experimental results on neutrino properties, in the context of this scenario, may be utilized to shed light on the bulk geometry (for phenomenological studies, see [4, 5, 8]).

In this paper we study this scenario based on the formalism of [9]. Our first aim is to determine whether a realistic neutrino spectrum can still be generated when the constraints on mixing angles between active and sterile neutrinos are taken into account, and particularly the severe constraint from the SNO experiment. Such constraints should indeed apply on the considered scenario, since the new right handed neutrino, as well as each component of its infinite massive tower of Kaluza-Klein (KK) excitations, constitute sterile neutrinos which mix with SM active neutrinos.

Our second goal is to address the issue of a successful leptogenesis within such realistic ED model in agreement with experimental neutrino data. More precisely, by studying the decays of the heavy KK neutrinos, we explore the possibilities that these scenarios account for the observed baryonic asymmetry of the Universe by means of the Fukugita-Yanagida mechanism of leptogenesis [10]. In this mechanism an excess of Lepton number ( $L$ ), generated by out-of-equilibrium  $L$ -violating decays of the heavy neutrinos, is converted into a Baryon number ( $B$ ) asymmetry through  $(B + L)$ -violating sphaleron interactions. At this stage we mention a preliminary work [6] where the leptogenesis has also been considered in the same context of flat extra dimensions, but with an extended Higgs sector compared to the SM and without considering the various experimental neutrino data.

We will consider the case where gravity may propagate in an higher dimensional space of  $[1 + (3 + n_g)]$  dimensions, where  $n_g \geq 1$ . Depending on this we have two variants of the scenario, one with  $n_g = 1$  and the other with  $n_g > 1$ . In all cases, the SM particles are localized on a  $[1 + 3]$  dimensional subspace (3-brane). For simplification reason, the sterile neutrinos are assumed to propagate in  $[1 + (3 + 1)]$  dimensions.

The organization of the paper is as follows. We begin with a brief outline of the essential features of the extra dimensional scenario in Sec 2. The relevant phenomenological constraints on neutrinos are discussed in Sec 3, while our numerical results are presented and discussed in Sec 4. Next in Sec 5, the issue of leptogenesis is addressed. Lastly, we summarize our studies, and conclude, in Sec 6.

## 2 Minimal Higher Dimensional Model for Neutrinos

In this section we describe the minimal ED framework with a 5-dimensional iso-singlet right handed neutrino added to the field content of the SM [4, 9]. Here, we stick to one generation of SM neutrinos. The fifth flat dimension, along which propagates the right handed neutrino, is compactified over a  $S^1/Z_2$  orbifold. The SM fields are localized on a 3-brane, whereas gravity propagates in the bulk.

The leptonic field content is,

$$L(x) = \begin{pmatrix} \nu_\ell(x) \\ \ell_L(x) \end{pmatrix}, \quad \ell_R(x), \quad (1)$$

as in the SM, where  $\nu_\ell$ ,  $\ell_L$ ,  $\ell_R$  are 4-dimensional Weyl spinors, plus the 5-dimensional singlet neutrino,

$$N(x, y) = \begin{pmatrix} \xi(x, y) \\ \bar{\eta}(x, y) \end{pmatrix}, \quad (2)$$

where  $y$  parameterizes the compact fifth direction, and  $\xi$ ,  $\eta$  are the 2-component spinors. The  $y$ -coordinate is compactified on a circle of radius  $R$  (the periodic boundary condition  $N(x, y) = N(x, y + 2\pi R)$  is imposed) on the singlet neutrino field. Additionally, under the action of  $Z_2$  symmetry, the two 2-component spinors may be associated with opposite parities,

$$\xi(x, y) = \xi(x, -y), \quad \eta(x, y) = -\eta(x, -y). \quad (3)$$

The SM fields are localized at the brane, which, just for generality, we may assume to be at  $y = a$ , instead of at the orbifold fixed point  $y = 0$ . The generic effective 4-dimensional Lagrangian of this model is given by,

$$\begin{aligned} \mathcal{L}_{\text{eff}} = & \int_0^{2\pi R} dy \left\{ \bar{N} \left( i\gamma^\mu \partial_\mu + \gamma_5 \partial_y \right) N - \frac{1}{2} \left( MN^T C^{(5)-1} N + \text{h.c.} \right) \right. \\ & \left. + \delta(y - a) \left[ \frac{h_1}{(M_F)^{1/2}} L \tilde{\Phi}^* \xi + \frac{h_2}{(M_F)^{1/2}} L \tilde{\Phi}^* \eta + \text{h.c.} \right] + \delta(y - a) \mathcal{L}_{\text{SM}} \right\}, \end{aligned} \quad (4)$$

where  $\tilde{\Phi} = i\sigma_2 \Phi^*$  is the hypercharge-conjugate of the SM Higgs doublet  $\Phi$ , with hypercharge  $Y(\Phi) = 1$ ,  $\mathcal{L}_{\text{SM}}$  is the SM Lagrangian,  $M$  is the Majorana mass for  $N$  (we do not specify its scale for the moment),  $C^{(5)}$  is the 5-dimensional charge conjugation operator and  $M_F$  is the fundamental  $n_g$ -dimensional gravity scale, given by

$$M_P = (2\pi M_F R)^{n_g/2} M_F, \quad (5)$$

for the simple case where all the compactification radii are of equal size  $R$ ,  $M_P$  being the 4-dimensional Planck scale. A Dirac mass term  $m_D \bar{N} N$  is not allowed in Eq.(4) because of the  $Z_2$  discrete symmetry.

Following Eq.(3), the 2-component spinors  $\xi$  and  $\eta$  can be expanded in Fourier series as,

$$\xi(x, y) = \frac{1}{\sqrt{2\pi R}} \xi_0(x) + \frac{1}{\sqrt{\pi R}} \sum_{n=1}^{\infty} \xi_n(x) \cos\left(\frac{ny}{R}\right), \quad (6)$$

$$\eta(x, y) = \frac{1}{\sqrt{\pi R}} \sum_{n=1}^{\infty} \eta_n(x) \sin\left(\frac{ny}{R}\right), \quad (7)$$

where the chiral spinors  $\xi_n(x)$  and  $\eta_n(x)$  form an infinite tower of KK fields. Using these expansions and integrating out the  $y$ -coordinate, the effective Lagrangian reduces to,

$$\begin{aligned} \mathcal{L}_{\text{eff}} = & \mathcal{L}_{\text{SM}} + \bar{\xi}_0(i\bar{\sigma}^\mu \partial_\mu) \xi_0 + \left( \bar{h}_1^{(0)} L \tilde{\Phi}^* \xi_0 - \frac{1}{2} M \xi_0 \xi_0 + \text{h.c.} \right) + \sum_{n=1}^{\infty} \left[ \bar{\xi}_n(i\bar{\sigma}^\mu \partial_\mu) \xi_n \right. \\ & + \bar{\eta}_n(i\bar{\sigma}^\mu \partial_\mu) \eta_n + \frac{n}{R} \left( \xi_n \eta_n + \bar{\xi}_n \bar{\eta}_n \right) - \frac{1}{2} M \left( \xi_n \xi_n + \bar{\eta}_n \bar{\eta}_n + \text{h.c.} \right) \\ & \left. + \sqrt{2} \left( \bar{h}_1^{(n)} L \tilde{\Phi}^* \xi_n + \bar{h}_2^{(n)} L \tilde{\Phi}^* \eta_n + \text{h.c.} \right) \right] \end{aligned} \quad (8)$$

in a basis in which  $M$  is positive, and with:

$$\bar{h}_1^{(n)} = \frac{h_1}{(2\pi M_F R)^{1/2}} \cos\left(\frac{na}{R}\right) = \left(\frac{M_F}{M_P}\right)^{1/n_g} h_1 \cos\left(\frac{na}{R}\right) = \bar{h}_1 \cos\left(\frac{na}{R}\right), \quad (9)$$

$$\bar{h}_2^{(n)} = \frac{h_2}{(2\pi M_F R)^{1/2}} \sin\left(\frac{na}{R}\right) = \left(\frac{M_F}{M_P}\right)^{1/n_g} h_2 \sin\left(\frac{na}{R}\right) = \bar{h}_2 \sin\left(\frac{na}{R}\right). \quad (10)$$

For deriving the last two equalities on the right hand sides of Eqs.(9)-(10), we have made use of Eq.(5).

Eqs.(9) and Eq.(10) tell us that the reduced 4-dimensional Yukawa couplings  $\bar{h}_{1,2}^{(n)}$  can be suppressed by many orders depending on the hierarchy between  $M_P$  and  $M_F$ ; for example, if gravity and the bulk neutrino feel the same number of extra dimensions, say  $n_g = 1$ , then these couplings are suppressed by a factor  $M_F/M_P \sim 10^{-15}$ , for  $M_F \approx 10$  TeV (see also [4, 5]).

From Eq.(2) we observe that  $\xi$  and  $\bar{\eta}$  have the same lepton number. Thus, the simultaneous presence of the two operators  $L\tilde{\Phi}^*\xi$  and  $L\tilde{\Phi}^*\eta$  in Eq.(8) leads to lepton number violating processes with  $\Delta L = 2$ . If the brane were located at one of the two orbifold fixed points ( $y = 0$  or  $\pi R$ ), the operator  $L\tilde{\Phi}^*\eta$  would have been absent in Eq.(8) as a consequence of the discrete  $Z_2$  symmetry. The two operators can coexist, leading to breaking of the lepton number, if we allow the brane to be shifted by an amount  $a (\neq 0)$  from the orbifold fixed points. In fact, it is possible to perform such a shifting of the brane (even in a continuous way) respecting the  $Z_2$  invariance of the original higher dimensional Lagrangian under certain restrictions in Type-I string theories [11]. As indicated in [4, 9], the  $Z_2$  invariance can be taken care of by allowing the replacements,

$$\begin{aligned}\xi \delta(y-a) &\rightarrow \frac{1}{2} \xi \left[ \delta(y-a) + \delta(y+a-2\pi R) \right], \\ \eta \delta(y-a) &\rightarrow \frac{1}{2} \eta \left[ \delta(y-a) - \delta(y+a-2\pi R) \right],\end{aligned}\tag{11}$$

with  $0 \leq a < \pi R$  and  $0 \leq y \leq 2\pi R$ . Obviously, a  $Z_2$ -invariant implementation of brane-shifted couplings would require the existence of at least two branes placed at  $y = a$  and  $y = 2\pi R - a$ . The non-zero shifting of the brane may turn out to be an important parameter for leptogenesis, to be tuned to generate breaking of lepton number, which is a necessary ingredient to generate lepton asymmetry. Another important motivation for a brane shifted framework was pointed out in [9], where it has been shown that in such a framework it is possible to completely de-correlate the effective Majorana-neutrino mass  $\langle m \rangle$ , that is effectively measured, and the scale of light neutrino masses, as to have  $\langle m \rangle$  within an observable range.

Following the notations of reference [4], we now introduce the weak basis for the KK Weyl-spinors,

$$\chi_{\pm n} = \frac{1}{\sqrt{2}} (\xi_n \pm \eta_n),\tag{12}$$

followed by a rearrangement of  $\xi_0$  and  $\chi_n^\pm$  states, such that, for a given value of  $k$  (say,  $k = k_0$ ) the smallest diagonal entry of the neutrino mass matrix is

$$|\varepsilon| = \min \left( \left| M - \frac{k_0}{R} \right| \right) \leq 1/(2R).\tag{13}$$

In this new basis the reordered 4-component Majorana-spinor vector  $\Psi_\nu$  is the following,

$$\Psi_\nu^T = \left[ \begin{pmatrix} \chi_{\nu_\ell} \\ \bar{\chi}_{\nu_\ell} \end{pmatrix}, \begin{pmatrix} \chi_{k_0} \\ \bar{\chi}_{k_0} \end{pmatrix}, \begin{pmatrix} \chi_{k_0+1} \\ \bar{\chi}_{k_0+1} \end{pmatrix}, \begin{pmatrix} \chi_{k_0-1} \\ \bar{\chi}_{k_0-1} \end{pmatrix}, \dots, \begin{pmatrix} \chi_{k_0+n} \\ \bar{\chi}_{k_0+n} \end{pmatrix}, \begin{pmatrix} \chi_{k_0-n} \\ \bar{\chi}_{k_0-n} \end{pmatrix}, \dots \right]\tag{14}$$

while the effective Lagrangian for right handed neutrinos reduces to,

$$\mathcal{L}_{\text{kin}} = \frac{1}{2} \bar{\Psi}_\nu \left( i \not{\partial} - \mathcal{M}_\nu^{\text{KK}} \right) \Psi_\nu,\tag{15}$$

where  $\mathcal{M}_\nu^{\text{KK}}$  is the corresponding neutrino mass matrix given by,

$$\mathcal{M}_\nu^{\text{KK}} = \begin{pmatrix} 0 & m^{(0)} & m^{(-1)} & m^{(1)} & m^{(-2)} & m^{(2)} & \dots \\ m^{(0)} & \varepsilon & 0 & 0 & 0 & 0 & \dots \\ m^{(-1)} & 0 & \varepsilon - \frac{1}{R} & 0 & 0 & 0 & \dots \\ m^{(1)} & 0 & 0 & \varepsilon + \frac{1}{R} & 0 & 0 & \dots \\ m^{(-2)} & 0 & 0 & 0 & \varepsilon - \frac{2}{R} & 0 & \dots \\ m^{(2)} & 0 & 0 & 0 & 0 & \varepsilon + \frac{2}{R} & \dots \\ \vdots & \vdots & \vdots & \vdots & \vdots & \vdots & \ddots \end{pmatrix}.\tag{16}$$

The most important consequence of such a rearrangement is that the mass scale  $M$ , which we did not specify earlier but which could be as large as possible, is now replaced by the light mass scale  $\varepsilon$ . The mass entries in the first row and first column of matrix (16) are given by the relation,

$$m^{(n)} = \frac{v}{\sqrt{2}} \left[ \bar{h}_1 \cos\left(\frac{(n-k_0)a}{R}\right) + \bar{h}_2 \sin\left(\frac{(n-k_0)a}{R}\right) \right] = m \cos\left(\frac{na}{R} - \phi_h\right), \quad (17)$$

with,

$$m = \frac{v}{2} \sqrt{\frac{h_1^2 + h_2^2}{\pi M_F R}}, \quad (18)$$

$$\phi_h = \tan^{-1}\left(\frac{h_2}{h_1}\right) + k_0 \frac{a}{R}, \quad (19)$$

where  $v$  is the vacuum expectation value of the SM Higgs boson.

### 3 Constraints for a Realistic Spectrum

The neutrino spectra is obtained by diagonalizing the mass matrix  $\mathcal{M}_\nu^{\text{KK}}$  of Eq.(16). It has been shown in [9], for a one-generation case, that the eigenvalue equation for a restricted class of cases with  $a = \pi R/q$ , where  $q$  is an integer greater than 1, is easily tractable analytically. We have, in the generic case, solved the characteristic eigenvalue equation numerically to obtain the eigenvalues of  $\mathcal{M}_\nu^{\text{KK}}$ , sticking to the one-generation case. We have diagonalized the  $N \times N$  matrix of Eq.(16) for a  $N$  satisfying  $M_F > M_{\text{max}}$  (see end of the paragraph). We have systematically checked that the  $N$  value used constitutes a dimension at which the lightest eigenvalues converge and are completely stabilized (with increasing  $N$ ). We have performed a scan over the whole parameter space of the ED model described above in order to find the regions in agreement with basic experimental constraints on neutrinos. The total parameter space consists of  $R^{-1}$ ,  $\varepsilon$ , the complex Yukawa couplings  $h_1$  and  $h_2$ , the brane-shift parameter  $a$ , and the phase  $\phi_h$  defined in Eq.(19). From Eq.(5), the effective cut off scale  $M_F$  for a given  $R^{-1}$  is completely fixed for  $n_g = 1$ ; while for  $n_g > 1$ , it depends on  $n_g$  and the respective compactification radii (respecting  $M_F > M_{\text{max}}$ , where  $M_{\text{max}}$  is the mass of the heaviest neutrino eigenstate considered).

While scanning over the total parameter space described above in order to search for a realistic neutrino mass spectrum, we have to ensure several constraints described in the following;

- There exist phenomenological constraints on the mixing angles between active neutrinos and sterile ones. These constraints apply on the present model, as the 0-mode and KK excitations of the additional right handed neutrino behave exactly as sterile neutrinos – the right handed neutrino having no electroweak interactions (see e.g. [12]).

For instance, in a model with a unique sterile neutrino, and assuming for simplicity one lepton flavor, the mixing angle  $\theta_s$  between the active and sterile neutrino is constrained typically by  $\tan \theta_s^2 \lesssim 10^{-6} - 10^{-1}$  for  $\Delta m^2 \in [10^{-12} - 10^2] \text{ eV}^2$  ( $\Delta m^2$  being the mass eigenvalue squared difference) [13] from cosmological and astrophysical considerations combined with data from atmospheric, solar (including SNO), reactor and short base-line experiments. In the limiting case  $\Delta m^2 \gg \Delta m_{\text{sun}}^2 \sim 10^{-5} \text{ eV}^2$ , the SNO bound on the fraction of oscillating sterile neutrinos coming from the sun  $\eta_s = \sin^2 \theta_s / 2$  [13], becomes approximatively [14, 15]

$$\eta_s \lesssim 1.2 \times 10^{-1} \text{ at } 1\sigma. \quad (20)$$

Similarly, in our framework, one can also take as an approximation that the  $\chi_{k_0}$  state, whose mass  $\varepsilon$  is the first appearing as a diagonal matrix element in Eq.(16), is the only sterile neutrino that may not decouple from the active SM neutrino  $\nu_\ell$ . Indeed, by definition of  $\varepsilon$  in Eq.(13), the following  $\chi_{k_0 \pm n}$  states get larger and larger diagonal mass matrix elements  $\varepsilon \pm n/R$  and thus decouple more and more from  $\nu_\ell$ , given the symmetric structure of the mass matrix in Eq.(16). Therefore, under the above approximation, the SNO

bound on  $\theta_s$  apply in our framework also, where the mixing angle  $\theta_s$  is deduced only from the  $2 \times 2$  block matrix of Eq.(16):

$$\tan 2\theta_s \approx \frac{2m^{(0)}}{\varepsilon}. \quad (21)$$

The above SNO bounds impose a significant upper limit on  $\theta_s$  leading to a case comparable to the see-saw mechanism (see also the third point) so that the smallest eigenvalue  $m_{\nu_1}$  and the next-to-smallest eigenvalue  $m_{\nu_2}$  read as

$$m_{\nu_1} \approx \frac{m^{(0)}}{\varepsilon} m^{(0)}, \quad m_{\nu_2} \approx \varepsilon. \quad (22)$$

The constraint in Eq.(20) imposes  $m^{(0)} \ll \varepsilon$  (*c.f.* Eq.(21)), which may be achieved in the following two cases (see Eq.(17)):

$$m \ll \varepsilon, \quad \text{and/or} \quad \phi_h \simeq \pi/2 + 2q\pi, \quad (23)$$

where  $q$  is an integer.

- Due to the see-saw structure of the mass matrix, the two eigenstates  $\nu_1$  and  $\nu_2$  are respectively composed mainly by the SM neutrino  $\nu_\ell$  and sterile state  $\chi_{k_0}$ . Hence one can apply the phenomenological bound on  $m_{\nu_1}$  derived for SM neutrinos, which in the case of one flavor is typically [17]

$$m_{\nu_1} \sim 10^{(-2, 0)} \text{ eV}. \quad (24)$$

- We have also ensured that the mass of the next-to-lightest<sup>1</sup> eigenstate  $\nu_2$  is larger than the mass of the Higgs boson, typically

$$m_{\nu_2} \geq 200 \text{ GeV}, \quad (25)$$

for our purpose which deals with its possible lepton-number violating decay into Higgs and leptons:  $\nu_2 \rightarrow \ell^\pm \phi^\mp$  (the three-body decay channel of the  $\nu_2$  is  $\nu_2 \rightarrow \ell^\pm \ell^\mp \nu_1$ ).

The choice of this condition  $m_{\nu_2} > 200 \text{ GeV}$  is important for our study of leptogenesis (in Sec 5). We could also have imposed this constraint on any higher-mass neutrino eigenstate  $m_{\nu_i} > 200 \text{ GeV}$  with  $i > 2$ , and studied the decay  $\nu_i \rightarrow \ell^\pm \phi^\mp$ . However, any higher state  $\nu_i$  ( $i > 2$ ), in addition to its decay channel  $\nu_i \rightarrow \nu_1 \ell^+ \ell^-$ , possesses several other decay channels: their decays into lighter eigenstates  $\nu_i \rightarrow \nu_j \ell^+ \ell^-$  or  $\nu_i \rightarrow \nu_j \nu_1 \nu_1$  with  $i > j \geq 2$ . How the presence of these additional decay channels is going to affect the Boltzmann equations and the washout factors, and thus the resulting lepton abundance, is a matter of non-trivial calculation that we will not address here. Such additional decay channels do not exist for the state  $\nu_2$ , as the decays  $\nu_2 \rightarrow \nu_2 \nu_1 \nu_1$  and  $\nu_2 \rightarrow \nu_2 \ell^+ \ell^-$  are not possible kinematically. Here we consider the possibility of the ED model to yield a successful leptogenesis via the  $\nu_2$  decay.

With this bound  $m_{\nu_2} \geq 200 \text{ GeV}$  we are in the case where  $\Delta m^2 = m_{\nu_2}^2 - m_{\nu_1}^2 \gg \Delta m_{sun}^2$  so that the relevant SNO bound is the one given in Eq.(20). Furthermore, this condition forces  $m_{\nu_2}$  to be much larger than  $m_{\nu_1}$  and so constitutes another justification for approximating the two lightest eigenvalues by the see-saw formulas (22).

At this stage the following remarks on neutrino mass are in order. There are typically three different mass suppression mechanisms in the extra dimensional scenario, that may suppress the mass of the SM neutrino.

1. The usual see-saw like suppression, from a heavy Majorana mass  $M$  for the right handed neutrino.
2. An effective ED see-saw type mechanism resulting from the massive KK tower [4, 6], where the KK excitations of the additional right handed neutrino play the rôle of the right handed neutrino in the usual see-saw mechanism.
3. A suppression of the Yukawa couplings from the ED wavefunction overlap mechanism affecting the neutrino mass via the ED volume factor  $(M_F R)^{1/2}$  (see Eq.(18)) and the factor  $\cos(na/R - \phi_h)$  (see Eq.(17)).

---

<sup>1</sup>In our notations we order the mass eigenvalues increasingly, i.e.  $m_{\nu_1} \leq m_{\nu_2} \leq \dots$ .

The main motivation for working in an ED scenario is to generate small SM neutrino masses using the second and third mechanisms only, i.e. the usual see-saw mechanism does not constitute the main suppression origin. Is that possible? As we have already discussed, the diagonal matrix element  $\varepsilon$  contributes dominantly to the eigenvalue  $m_{\nu_1}$  since it is the lightest one. Hence in order to insure that the neutrino mass suppression is not mainly due to the usual see-saw mechanism, one can impose the condition  $M \neq \varepsilon$ , which is equivalent to  $M > 1/2R$  (see upper left  $2 \times 2$  block matrix in Eq.(16)). This condition can always be satisfied since the mass scale  $M$  never appears in this scenario directly: the presence of the infinite tower of KK states guarantees that only the value of  $M$  modulo  $R^{-1}$ , namely  $\varepsilon$  (in absolute values) plays a physical rôle [4, 9].

We now discuss the ranges considered for each fundamental free parameter. First we made sure that it is mainly the second and/or the third mechanism (described previously) that suppresses  $m_{\nu_1}$ , by letting the numerical values of the Yukawa couplings  $h_1$  and  $h_2$  to be within the natural range  $\sim 0.1 - 5$  with the respective phases ranging between 0 and  $\pi$ . The phase  $\phi_h$  was also varied within 0 and  $\pi$ . We varied  $R^{-1}$  from a few tens of eV up to  $\sim 10^{19}$  GeV. For  $R^{-1} \gtrsim 10^{19}$  GeV, the heaviest state considered has a mass  $M_{\max}$  greater than  $M_F$ , i.e. our low energy effective theory loses its predictivity. The range of  $R^{-1}$  being so huge, we considered a logarithmic binning of the scale of  $R^{-1}$ . For each  $R^{-1}$ , the parameter  $\varepsilon$  may also vary within a large range, especially when  $R^{-1}$  is large, following Eq.(13). So we also scan over  $\varepsilon$  by choosing randomly the values of  $\alpha$  in  $\varepsilon = 10^\alpha$ . The brane shift parameter  $a$  was scanned in a similar way in  $0 < a < \pi R$ . Finally, we performed a scan by *randomly* choosing  $\sim 10^6$  points, so that each point corresponds to a *distinct but random* combination of all the parameters.

## 4 Results and Discussion

When scanning over the parameter space  $\{R^{-1}, \varepsilon, \phi_h, h_1, h_2, a\}$  we have imposed a realistic spectra, i.e. one respecting all the constraints mentioned in the previous section. We have explored the two situations allowing for such realistic spectra (*c.f.* Eq.(23)) within two scenarios characterized by  $n_g = 1$  and  $n_g > 1$ . Our observations and discussion for both the scenarios are given below. We have also included, in each case, possible analytical interpretations of our results.

### 4.1 Scenario with $n_g = 1$

1. **The scale  $M_F$ :** We recall (see Eq.(5)) that the cut off scale  $M_F$  depends only on  $R^{-1}$  for  $n_g = 1$ . As we increase the scale of  $R^{-1}$  from a few tens of eV to  $\sim 10^{19}$  GeV, the corresponding scale  $M_F$  increases from  $\sim 10^9$  GeV to  $\sim 10^{19}$  GeV, following Eq.(5). This makes the scale  $m$  in Eq.(18) increasing from  $\sim 10^2$  eV to  $\sim 10^3$  GeV.
2. **The parameter  $R^{-1}$ :** We observed that the energy scale  $R^{-1}$  has to be  $\gtrsim 400$  GeV (corresponding to  $M_F \gtrsim 10^{13}$  GeV) for generating a realistic neutrino spectrum (see Fig.1). The reason is that  $R^{-1} \geq 2|\epsilon|$  (from Eq.(13)) with  $\epsilon \approx m_{\nu_2}$  from Eq.(22) and we have imposed  $m_{\nu_2} \geq 200$  GeV. With regard to the neutrino mass, what is the physical meaning of this lower bound on  $R^{-1}$ ? We know from Eq.(5), that as  $R^{-1}$  increases,  $M_F$  also increases but at a much slower rate compared to  $R^{-1}$ . As a result, the quantity  $1/\sqrt{M_F R}$  increases with  $R^{-1}$  so that the volume suppression mechanism for Yukawa couplings becomes less and less effective (see Eqs.(9), (10)), for a fixed  $\cos \phi_h$ . Besides, the hierarchy between  $m^{(0)} \propto 1/\sqrt{M_F R}$  and  $R^{-1}$  increases with  $R^{-1}$ , so that the effective ED see-saw mechanism becomes more effective in the reduction of  $m_{\nu_1}$  if  $\varepsilon$  is set at its maximum value  $1/2R$ . Indeed the denominator of  $m_{\nu_1}$  (Eq.(22)) clearly increases at a faster rate compared to the numerator  $m^{(0)}$  - thus making the see-saw formulae more effective as  $R^{-1}$  increases. Therefore, the fact that there is a minimum value for  $R^{-1}$  means that the see-saw mechanism plays at least a certain rôle in the neutrino mass suppression.
3. **The parameter  $\varepsilon$ :** For all  $R^{-1} \gtrsim 400$  GeV, there exists a minimum value of  $\varepsilon$ , starting from which we end up with a realistic spectrum for all possible higher values of  $\varepsilon$  ( $\leq 1/2R$ ). This minimum value is

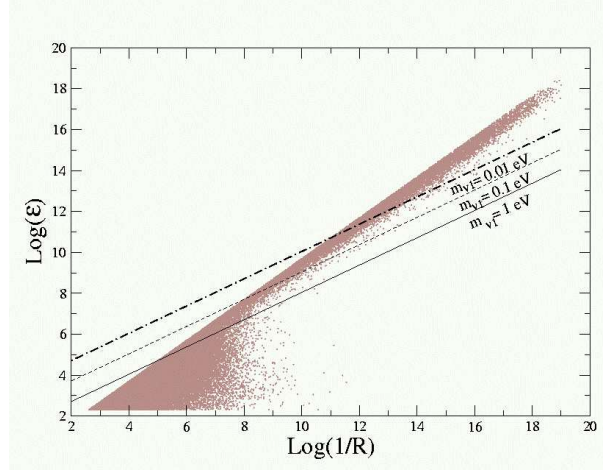


Figure 1: Plot of  $\varepsilon$  (in GeV) versus  $1/R$  (in GeV) obtained from the scan. The three straight lines represent the analytical approximation of Eq.(22) for the indicated values of  $m_{\nu_1}$ .

significantly larger than 200 GeV (recall that  $\varepsilon \approx m_{\nu_2} \geq 200$  GeV) for  $1/R \gtrsim 10^8$  GeV, as we see on Fig.1 which shows the plot of  $\varepsilon$  versus  $1/R$ . This can be understood as follows.

This figure results from the general scan, and thus includes both the cases  $m \ll \varepsilon$  and  $\phi_h \sim \pi/2 + 2q\pi$ . The three straight lines correspond to the  $\varepsilon$  values obtained analytically from the approximate see-saw relation in Eq.(22), for  $m_{\nu_1} = 1$  eV, 0.1 eV and 0.01 eV, and  $\sqrt{h_1^2 + h_2^2} = 4$  and  $\phi_h = 0$  (i.e.  $\cos \phi_h = 1$ ). Therefore, the points obtained close to these lines correspond to the case where the  $m_{\nu_1}$  suppression is mainly due to the configuration (1). The regions far below these lines indicate the simultaneous occurrence of both configuration (1) and (2) i.e.  $m \ll \varepsilon$  as well as  $\phi_h \sim \pi/2 + 2q\pi$ . Starting from these regions and approaching higher  $R^{-1}$  values,  $m$  increases, making the  $m_{\nu_1}$  suppression from (1) less effective. Thus if we are to generate the same amount of suppression in  $m_{\nu_1}$  (or equivalently the same smallness of ratio  $m^{(0)}/\varepsilon$ ) for a fixed  $\varepsilon$ , the  $m_{\nu_1}$  suppression coming from case (2) must be more effective, i.e.  $\phi_h$  has to be closer to  $\pi/2$ . This condition on  $\phi_h$  basically reduce the allowed range for  $\phi_h$ , so that the scan misses the allowed  $\phi_h$  values. This explains the large vacant area in Fig.1 below the three lines. Therefore, the easier way to generate the suppression in the higher  $R^{-1}$  region is by case (1), i.e. by pushing the minimum value of  $\varepsilon$  to be still higher to account for the increase in  $m$ . Quite naturally therefore, the available parameter region for higher  $R^{-1}$  decreases, and is concentrated near maximal values of  $\varepsilon$ .

4. **The parameters  $\phi_h$  and  $a$ :** First let us discuss the spectrum. Since we are always working in a parameter region such that the off-diagonal elements of the mass matrix of Eq.(16) are much smaller than the diagonal elements, the eigenvalues  $m_{\nu_i}$  of the matrix, up to a good approximation (see the appendix), are equal to the diagonal elements for  $i \geq 2$ :  $m_{\nu_2} \sim \varepsilon$ ,  $m_{\nu_3} \sim \varepsilon - 1/R$ ,  $m_{\nu_4} \sim \varepsilon + 1/R$ , and so on. In general, the masses of the higher neutrino states can be expressed as  $m_{\nu_{(2p+1)}} \sim \varepsilon - p/R$ ,  $m_{\nu_{(2p+2)}} \sim \varepsilon + p/R$ , where  $p$  is an integer  $\geq 1$ . This clearly tells us that for a given  $R^{-1}$ , the nature of the resulting spectra is *primarily* dictated by the choice of  $\varepsilon$ . For example, if  $\varepsilon = 1/2R$ , the resulting spectrum becomes almost pairwise degenerate with  $|m_{\nu_2}| \sim |m_{\nu_3}|$  (see Eq.(22)),  $|m_{\nu_4}| \sim |m_{\nu_5}|$ , and so on, while, for all the other choices of  $\varepsilon$ , the resulting spectrum is hierarchical with  $m_{\nu_2} < m_{\nu_3} < m_{\nu_4} < m_{\nu_5} < \dots$ .

In particular, we found that for a given  $R^{-1}$ , the overall nature of the resulting spectrum *feebly* depends on the choice of the parameters  $\phi_h$  and  $a$ . This is expected since these parameters appear *only* in the non-diagonal mass-matrix elements which are much smaller than the diagonal ones for any  $\phi_h$  and  $a$  values (as those enter via arguments of a cosine function). For example, it was found that for any  $R^{-1} \gtrsim 400$  GeV, if  $\varepsilon \sim 1/2R$ , then *all* possible combinations of  $\phi_h$  and  $a$  yield realistic spectra. Naturally, these possible combinations of  $\phi_h$  and  $a$  include  $a = 0$  as well. For possible lower values of  $\varepsilon$ , which may not correspond to  $m \ll \varepsilon$ , a realistic spectra was obtained, quite expectedly, from the second case  $\phi_h \sim \pi/2 + 2q\pi$ . Note that for this case also,  $a = 0$  and  $\phi_h \sim \pi/2$  is a natural possibility, and our scan selects indeed this



combination. Thus the important conclusion that we made from these observations was that a non-zero brane-shift is *not essential* for a realistic mass spectrum.

Let us compare our observations with those of Ref.[9].

The authors of reference [9] found that when  $\varepsilon = 0$ ,  $\phi_h = 0$  and  $a = 0$ , the mass spectra consists of massive pairwise degenerate neutrino states without any massless state. They also found that when  $\varepsilon = 1/2R$ ,  $\phi_h = 0$  and  $a = 0$ , there is an almost massless state, and the remaining spectra consists of pairwise degenerate massive neutrino states. We have found the same observation for these two points.

They further found that when  $\varepsilon \neq 0$  and  $\neq 1/2R$ ,  $\phi_h = 0$  and  $a = 0$ , there is no massless state and the mass spectra is hierarchical. We indeed find an *almost massless* neutrino state in this case too, the overall spectrum being hierarchical.

They also found that *unless*  $\varepsilon = 1/2R$ ,  $\phi_h = \pi/4$  and  $a = \pi R/2$ , the mass spectrum consists of massive non-degenerate KK neutrinos. We find indeed that for  $\varepsilon = 1/2R$ ,  $\phi_h = \pi/4$  and  $a = \pi R/2$ , the high neutrinos states are pairwise degenerate.

However, we found that for several other combinations of these three parameters one can also get a realistic mass spectrum. For example, we mentioned before that for  $\varepsilon = 1/2R$ , we always get the spectra consisting of an almost massless state and other states pairwise degenerate, irrespective of the numerical values of  $\phi_h$  and  $a$ . Our larger allowed domain of parameter space is due to the additional de-correlation condition required in [9], and not considered here. In particular, a non-zero brane-shift parameter is found to be necessary in [9] in order to account for this complete de-correlation of the effective Majorana mass term  $\langle m \rangle$  and the scale of light neutrino mass (the motivation being to have  $\langle m \rangle$  in a potentially observable range). In contrast, we find the brane-shift to be not essential for a realistic mass spectrum.

5. **The quantity  $m^{(0)}$ :** We finish this section by determining which of the two possible ED mechanisms responsible for the suppression of  $m_{\nu_1}$  (discussed in Sec3) plays the dominant rôle (for different values of  $R^{-1}$ ). Our discussion is based on the plot of  $m^{(0)}/\varepsilon$  versus  $\varepsilon$  in Fig.2. One first observes clearly from the figure that systematically  $m^{(0)} \leq 10^{-5}\varepsilon$  which means that the effective ED see-saw mechanism plays *always* a significant rôle in reducing  $m_{\nu_1}$  (see Eq.(22)), as we have already noticed. One see typically that the  $m_{\nu_1}$  suppression, relative to the electroweak symmetry breaking scale ( $v \sim 10^2$  GeV), can be due at 50% from the effective ED see-saw mechanism and at 50% from the higher dimensional mechanism based on wave function overlap, a situation corresponding to  $\varepsilon \sim 10^2$  GeV and  $m^{(0)} \sim 10^{-3}$  GeV (such that  $m^{(0)}/v \sim m^{(0)}/\varepsilon \sim 10^{-5}$ ). The suppression can even come *purely* from the effective ED see-saw mechanism, namely  $m^{(0)}/\varepsilon \sim 10^{-11}$  with  $m^{(0)} \sim v \sim 10^2$  GeV. Thus the fact that  $m^{(0)}/\varepsilon \lesssim 10^{-5}$  means that the ED see-saw mechanism is systematically the dominant one.

This can interpreted in the following terms. All the conditions that we have imposed resulted in a lower bound on  $R^{-1}$  (see above)<sup>2</sup>. Now, as  $R^{-1}$  increases, the extra compact bulk space decreases, so that the wavefunction overlap factor increases, making the suppression of  $m_{\nu_1}$  from the geometrical mechanism less effective. Hence, the different constraints (including the SNO one) limit the wave function overlap mechanism effect. Nevertheless, thanks to the ED see-saw mechanism, a realistic spectrum can still be generated.

## 4.2 Results for the $n_g > 1$ scenario

We consider now another scenario where the right handed neutrino propagates only along one extra dimension whereas gravity propagates in the whole bulk, the number  $n_g$  and sizes of extra dimensions being adjusted (with Eq.(16) when all of them have the same size  $2\pi R$ ) such that  $M_F$  is as low as  $\sim \mathcal{O}(1)$  TeV in order to address the gauge hierarchy problem. Recall that the solution to the gauge hierarchy problem within the ADD model for  $n_g = 1$  is excluded by experimental arguments relative to the Newton law modification<sup>3</sup>.

<sup>2</sup>In particular, the SNO bound constrains the mixing angles between active and sterile neutrinos, by this way forcing typically the KK masses ( $\propto 1/R$ ) to increase.

<sup>3</sup>In our case for the  $n_g = 1$  scenario, the cutoff scale was set around  $10^{13}$  GeV and more. This model, for sure, did not address the gauge hierarchy issue.

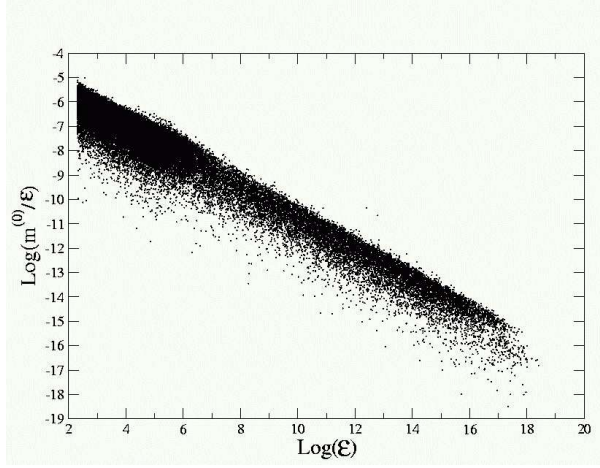


Figure 2: Plot of  $m^{(0)}/\varepsilon$  versus  $\varepsilon$  (in GeV).

The radius, as found previously, is bounded from above by  $R^{-1} \gtrsim 400$  GeV, since  $R^{-1} \geq 2|\varepsilon|$ ,  $\varepsilon \approx m_{\nu_2}$  and  $m_{\nu_2} \geq 200$  GeV. As a consequence,  $m^{(0)} \sim v/\sqrt{M_F R} \gtrsim 10^2$  GeV<sup>4</sup> as  $M_F \sim \mathcal{O}(1)$  TeV, so that there is no significant suppression in  $m^{(0)}$  (and hence in  $m_{\nu_1}$ ), relative to the electroweak scale  $v$ , coming from the ED overlap mechanism. Thus the neutrino mass suppression must originate principally from the ED see-saw mechanism. For that purpose, one should have  $m^{(0)}/\varepsilon \sim 10^{-11}$  (see Eq.(22)) which together with  $m^{(0)} \sim v/\sqrt{M_F R}$  and  $|\varepsilon| < 1/2R$  leads to  $R^{-1} \gtrsim 10^{26}$  GeV: an amount much larger than the fundamental scale  $M_F \sim \mathcal{O}(1)$  TeV. Thus, for the  $n_g > 1$  scenario, generating a realistic neutrino spectrum and addressing the gauge hierarchy issue simultaneously, is only possible if there exists a compactification scale  $1/R$  extremely different from the fundamental scale  $M_F$  (hence another hierarchy has to be introduced). Besides, such a scenario is automatically in a non-predictable regime, since the condition  $M_{\max} < M_F$  translates into  $1/R \lesssim$  TeV.

## 5 Leptogenesis

One interesting question to address is the possibility of having successful leptogenesis in these ED scenarios. As has been argued in [6], the infinite KK tower of neutrinos associated with the 5-dimensional sterile neutrino may act as an infinite series of CP-violating resonators. Thus, we probed the ED scenarios to see whether they can generate sufficient lepton asymmetry.

### 5.1 Additional Constraints and Expectations

In the previous section we saw that the lightest neutrino  $\nu_1$  in the generated spectrum fulfills the absolute scale bound. We also constrained the next to lightest neutrino  $\nu_2$  to be heavier than the Higgs mass, so that it may decay at a temperature corresponding to its mass and produce lepton asymmetry [10]. The out-of equilibrium condition may be written as the following condition on the decay width of  $\nu_2$ ,

$$\Gamma_{\nu_2} \simeq \frac{K_{22} m_{\nu_2}}{8\pi} < H(T = m_{\nu_2}), \quad K_{jj} \equiv [\lambda^\dagger \lambda]_{jj}, \quad (26)$$

where  $H$  is the Hubble expansion rate at  $T = m_{\nu_2}$ , and  $\lambda_j$  is the modified Yukawa coupling for the neutrino mass eigenstate  $\nu_j$ . The initial Yukawa couplings,  $\lambda'$ , can be read from Eq.(17):  $m^{(j)} = \lambda'_j v/\sqrt{2}$ . When the

<sup>4</sup>Unless of course  $\phi_h \sim \pi/2 + 2q\pi$ , but in order to decrease significantly the order of magnitude of this lower bound on  $m_{(0)}$ ,  $\phi_h$  should be extremely close to  $\pi/2 + 2q\pi$  which has a priori no theoretical justification.

complex symmetric mass matrix in Eq.(16) is diagonalized, the weak states  $\Psi_\nu$  of Eq.(14) transform to the mass eigenstates  $\Psi^{\text{mass}}$  following  $\Psi_\nu = V\Psi_\nu^{\text{mass}}$ , where  $V$  is the diagonalizing matrix. Thus the initial Yukawa couplings for right handed neutrinos  $\lambda'_i$  also transform into the modified Yukawa couplings  $\lambda_j$  via the  $V$  matrix. We note the Yukawa couplings  $\lambda_i$  instead of  $\lambda_{i1}$ , where the index 1 is fixed as it corresponds to the unique left handed SM lepton (we remind that we work under the simplification assumption of one family) which moreover does not develop a KK tower. The condition in Eq.(26) is the first filter to ensure a successful thermal leptogenesis. The other necessary condition is to generate enough CP asymmetry, the asymmetry being defined by,

$$\epsilon_{\text{CP}} = \frac{\Gamma(\nu_2 \rightarrow \ell\phi) - \Gamma(\nu_2 \rightarrow \bar{\ell}\bar{\phi})}{\Gamma(\nu_2 \rightarrow \ell\phi) + \Gamma(\nu_2 \rightarrow \bar{\ell}\bar{\phi})}, \quad (27)$$

This asymmetry gets a non-zero value due to the interference between the tree level diagram of Fig.3a and one-loop diagrams of Fig.3b and 3c. The asymmetry is given by,

$$\epsilon_{\text{CP}} = \frac{1}{8\pi K_{22}} \sum_{j \neq 2} \text{Im}[K_{2j}^2] f(m_{\nu_j}^2/m_{\nu_2}^2), \quad (28)$$

where  $f$  is the loop factor [18], given by

$$f(x) = \sqrt{x} \left[ 1 - (1+x) \ln \frac{1+x}{x} + \frac{1}{1-x} \right], \quad (29)$$

in the case of a hierarchical neutrino spectrum. Here  $\nu_2$ , the next-to-lightest neutrino, is the external (i.e. decaying) mode and  $\nu_j$  the exchanged eigenstate (see Fig.3). The amount of CP asymmetry generated can be magnified by the loop function and/or the Yukawa couplings. However, due to the large hierarchy between the lightest first state  $\nu_1$  and the next-to-lightest state  $\nu_2$ , much enhancement from the Yukawa couplings cannot be expected, as we will discuss more precisely in the next subsection. The other enhancement may then come from the loop function via resonances. The discussion on the characteristics of the generated KK neutrino spectrum in the previous section clearly shows that we are indeed often in this favorable resonance situation ( $\Leftrightarrow \varepsilon \sim 1/2R$ ), since the neutrino eigenstates are almost pairwise degenerate over a wide range of the obtained parameter space. In this situation, the self energy contribution to the loop factor, which is the last term in Eq.(29), is modified to [19]

$$f^{\text{res}}(m_{\nu_j}^2/m_{\nu_2}^2) = \frac{(m_{\nu_2}^2 - m_{\nu_j}^2)m_{\nu_2}\Gamma_{\nu_j}}{(m_{\nu_2}^2 - m_{\nu_j}^2)^2 + m_{\nu_2}^2\Gamma_{\nu_j}^2}, \quad (30)$$

where  $\Gamma_{\nu_j} \simeq K_{jj}m_{\nu_j}/8\pi$  is the decay width of state  $\nu_j$ .

## 5.2 Results and Discussion

As before, we have scanned the total parameter space with the additional constraints mentioned above concerning leptogenesis, concentrating on the scenario with  $n_g = 1$ . We checked that within the previously obtained parameter space, the first test to ensure leptogenesis (represented by Eq.(26)), is satisfied.

As shows Eq.(28), the source of a non-zero CP asymmetry is the difference of phases of the Yukawa couplings. Since we are working with one generation of neutrinos, there is a single (common) phase associated with the Yukawa couplings  $\lambda'$  (the one associated with the SM neutrino). However, the final (modified) Yukawa couplings  $\lambda_j$  may still be different for different neutrino mass eigenstates  $\nu_j$ , as  $V$  itself is a complex matrix. The resulting difference of phases, generated in the process of diagonalization of the mass matrix as described above, leads to a non-zero value of  $\text{Im}[\lambda^\dagger \lambda]_{2j}^2$ .

However, although non-zero,  $\text{Im}[\lambda^\dagger \lambda]_{2j}^2$  is small due to the large hierarchies among the elements of the mass matrix, which in turn is essential to generate a realistic neutrino spectrum with small active-sterile mixing angles. We find numerically that the resonance enhancement in  $\epsilon_{\text{CP}}$  from the loop function cannot compensates

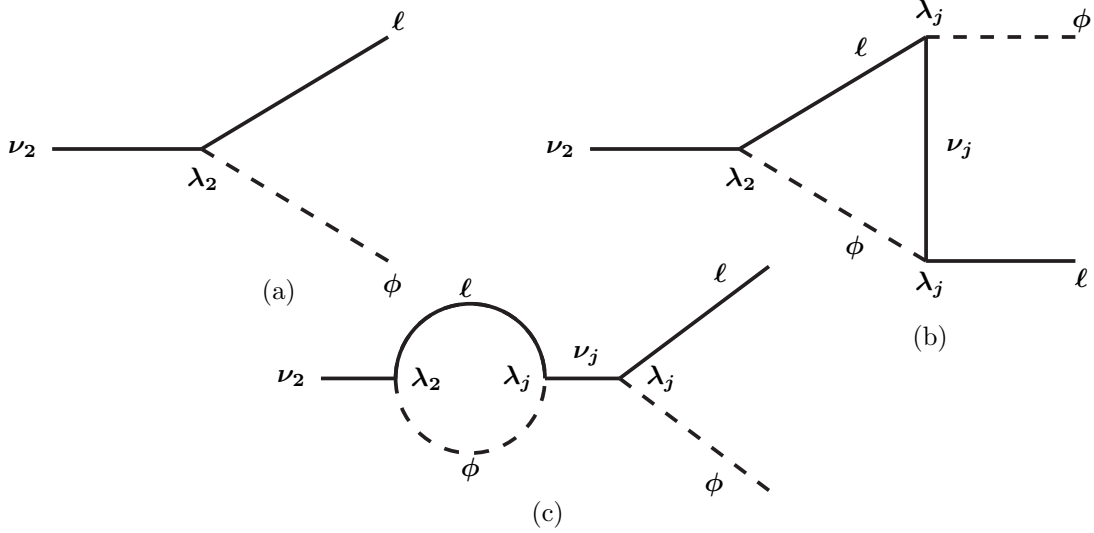


Figure 3: Diagrams for the CP-asymmetry decays, at tree (a) and loop (b)-(c) level, of the second neutrino eigenstate  $\nu_2$  into the charged lepton and the charged Higgs boson.

this suppression from the Yukawa couplings in order to ultimately generate a sufficient CP asymmetry for a successful leptogenesis:  $\epsilon_{\text{CP}} > 10^{-8}$  [20] (assuming the usual orders of magnitude for the washout factors). Thus, although the pairwise quasi-degenerate KK neutrino spectrum for one-generation of SM neutrino is favorable for yielding a good value of  $\epsilon_{\text{CP}}$ , but the suppression of the same from the Yukawa couplings turns out to be too dominant.

A possible alternative for a potentially successful leptogenesis could be to probe a more realistic model with three generations of SM neutrinos on the 3-brane, with three extra right handed neutrinos in the bulk. The mass matrix in Eq.(16) in that case would have a similar structure with  $h_1$  and  $h_2$  replaced by  $3 \times 3$  matrices in the flavor space. The masses of the  $n^{\text{th}}$  neutrino states would remain approximately the same for each generation and the differences in the masses of the three light neutrinos would only come from the Yukawa couplings. This initial difference in the Yukawa couplings could be enhanced further during the process of diagonalization of the mass matrix. This is in contrast to the one-generation case where we had to start from a single Yukawa coupling, and the process of matrix diagonalization was the *only* source to create a difference in the final Yukawa coupling phases. Therefore, we could expect a much larger contribution to the CP asymmetry from the  $\text{Im}[\lambda^\dagger \lambda]$  factor, compared to the one-generation case.

## 6 Conclusions

In this work, we have considered an extra dimensional scenario, with the SM particles localized on a 3-brane and an additional right handed neutrino propagating along an extra dimension, providing new mechanisms for suppressing the neutrino mass. We probed the possibilities of this model to account simultaneously for a realistic neutrino mass spectrum and a sufficient lepton asymmetry (from the decays of the KK neutrinos). We considered two variants of the above scenario.

The first is when this extra dimension is the only available one ( $n_g = 1$ ). Then there exist fundamental parameters which give rise to a neutrino spectrum respecting the experimental constraints, on neutrino masses and active-sterile neutrino mixings (like the SNO bounds). We have found that in this framework, the neutrino mass suppression originates dominantly from the ED see-saw mechanism and partially from the ED wave function overlap effect. In fact, the SNO data limit the effect of the wave function overlap but a sufficiently small neutrino mass can be generated thanks to the ED see-saw mechanism. For certain parameter domains,

the spectra in this scenario consists of pairwise quasi-degenerate heavy (KK) neutrinos, together with a light neutrino. We observed that under the constraints on neutrino masses that we have imposed, a “brane shifted” framework of the extra dimensional model is not essential for generating a realistic mass spectra. Also, the inverse radius of compactification has to be pushed to  $\sim 400$  GeV (or more). This in turn results in very tiny phase differences among the modified Yukawa couplings (after the process of mass matrix diagonalization) so that it is not possible to create a CP asymmetry large enough to insure a successful leptogenesis. Indeed, such a tininess is not sufficiently compensated by the enhancement from the resonant loop function (related to the decay of the KK neutrinos) which is due to the pairwise quasi-degeneracy property of the spectrum.

In the second variant where gravity can propagate in more extra dimensions ( $n_g > 1$ ), the fundamental gravity scale is reduced down to the TeV scale so that the gauge hierarchy problem is addressed through the ADD approach. We have found that in this framework, the neutrino mass suppression originates also primarily from the ED see-saw mechanism and the compactification scale is of an order of magnitude much larger than the fundamental gravity scale.

### Acknowledgments

We thank R. Singh for important clarifications and suggestions regarding several numerical aspects at different stages of this work. We are also grateful to G. Bhattacharyya for reading the manuscript and proposing important modifications. A. A. acknowledges support from the ANR-05-JCJC-0023-02 (project NEUPAC). A. A. and G. M. acknowledge support from the ANR-05-BLAN-0163-01 (project Phys@Col@Cos). P. D. thanks for the grant from the University of Paris-XI provided during the fulfillment of this project.

## Appendix

Here we intend to show analytically that when the eigenvalues ( $\mathcal{E}_n$  with  $n \geq 2$ ) of mass matrix (16) are taken equal to the diagonal elements, their correction are much smaller than the eigenvalues themselves. For that purpose, let us start with the  $4 \times 4$  form of Eq.(16),

$$\mathcal{M} = \begin{pmatrix} 0 & m^{(0)} & m^{(-1)} & m^{(1)} \\ m^{(0)} & \varepsilon & 0 & 0 \\ m^{(-1)} & 0 & \varepsilon - \frac{1}{R} & 0 \\ m^{(1)} & 0 & 0 & \varepsilon + \frac{1}{R} \end{pmatrix}. \quad (31)$$

All the obtained sets of parameters (see discussion on Fig.1) lead to a significant hierarchy in  $m/\varepsilon$  (case (1) of Eq.(23)). Hence the  $m^{(n)}$  values are systematically much smaller than  $\varepsilon$ , from Eq.(17), namely:  $m^{(n)} \ll \varepsilon$ . We can thus rewrite matrix in Eq.(31) as  $\mathcal{M} = \mathcal{M}_D + \mathcal{M}_I$ , where  $\mathcal{M}_D$  is the diagonal matrix constructed from  $\mathcal{M}$ , and  $\mathcal{M}_I$  is a perturbation matrix with no diagonal entries given as,

$$\mathcal{M}_I = \begin{pmatrix} 0 & m^{(0)} & m^{(-1)} & m^{(1)} \\ m^{(0)} & 0 & 0 & 0 \\ m^{(-1)} & 0 & 0 & 0 \\ m^{(1)} & 0 & 0 & 0 \end{pmatrix}. \quad (32)$$

The zeroth order eigenvalues  $\mathcal{E}_i$  of  $\mathcal{M}$  can be written as,  $\mathcal{E}_1 = 0, \mathcal{E}_2 = \varepsilon, \mathcal{E}_3 = \varepsilon - 1/R, \mathcal{E}_4 = \varepsilon + 1/R$ . Since  $\mathcal{M}_I$  has all diagonal elements equal to zero, the lowest order correction to the eigenvalues reads as,

$$\delta\mathcal{E}_n = \sum_{n' \neq n} \frac{(\langle \psi_n | \mathcal{M}_I | \psi_{n'} \rangle)^2}{\mathcal{E}_n - \mathcal{E}_{n'}}, \quad (33)$$

where the  $\psi$ 's are the zeroth order eigenvectors (considering the non-degenerate case). Thus, for our case we have from the above relations,

$$\delta\mathcal{E}_1 = \frac{(m^{(0)})^2}{-\varepsilon} + \frac{(m^{(1)})^2}{-\varepsilon - 1/R} + \frac{(m^{(-1)})^2}{-\varepsilon + 1/R} \quad (34)$$

(35)

$$\delta\mathcal{E}_n = (m^{(n)})^2/\mathcal{E}_n, \quad (36)$$

where  $m^{(n)}$  is given by Eq.(17) and  $n > 1$ . Since  $m \ll \varepsilon$ , the first two of the above relations lead to

$$\delta\mathcal{E}_1 \leq m^2 \left[ \frac{2\varepsilon}{(1/R)^2 - (\varepsilon)^2} - \frac{1}{\varepsilon} \right], \quad (37)$$

$$\delta\mathcal{E}_2 \leq m^2/\varepsilon. \quad (38)$$

These inequalities can immediately be generalized to the  $N \times N$  mass-matrix as,

$$\delta\mathcal{E}_1 \leq m^2 \left[ \sum_{n=1}^{(N-1)/2} \frac{2\varepsilon}{(n/R)^2 - (\varepsilon)^2} - \frac{1}{\varepsilon} \right], \quad (39)$$

$$\delta\mathcal{E}_2 \leq m^2/\varepsilon. \quad (40)$$

For the maximum value of  $\varepsilon$  ( $= 1/2R$ ), the first term on the right hand side of Eq.(39) is  $\sim 2R$  for large  $N$ , so that  $\delta\mathcal{E}_1 \sim 0$ . For smaller values of  $\varepsilon$ ,  $\delta\mathcal{E}_1$  would be dominated by the second term on right hand side. For all the other eigenvalues with  $n > 2$ , one can derive  $\mathcal{E}_n \geq \varepsilon$ . Thus, in general the numerical value of  $\delta\mathcal{E}_n$  for *any*  $n$  verifies

$$|\delta\mathcal{E}_n| \leq m^2/\varepsilon. \quad (41)$$

So let us study the  $m^2/\varepsilon$  value. For  $R^{-1} \lesssim 10^8$  GeV,  $\varepsilon \gtrsim 200$  GeV (see Fig.1) and  $m \lesssim 10^{-1}$  GeV (*c.f.* Eq.(18) and Eq.(5) in case of the scenario with  $n_g = 1$ ). Hence, one has  $m^2/\varepsilon \lesssim 10^{-5}$  GeV. Now for  $R^{-1} \gtrsim 10^8$  GeV,  $\varepsilon \sim R^{-1}/2$  and  $m \sim 10^{-4} (R^{-1}/1\text{GeV})^{1/3}$  GeV, so that  $m^2/\varepsilon \sim 10^{-8} (R^{-1}/1\text{GeV})^{-1/3}$  GeV and thus  $m^2/\varepsilon \lesssim 10^{-11}$  GeV. Therefore, from Eq.(41), we conclude that one has systematically  $|\delta\mathcal{E}_n| \ll \mathcal{E}_n$  for each  $n \geq 2$ , since  $\mathcal{E}_{n \geq 2} \gtrsim \varepsilon \gtrsim 200$  GeV. A similar analysis could be performed for the case of the degenerate mass spectra (then we would have to start from the corresponding relation of Eq.(33) for degenerate eigenvalues).

## References

- [1] N. Arkani-Hamed, S. Dimopoulos and G. Dvali, Phys. Lett. B **429** (1998) 263; I. Antoniadis, N. Arkani-Hamed, S. Dimopoulos and G. Dvali, Phys. Lett. B **436** (1998) 257; K.R. Dienes, E. Dudas and T. Gherghetta, Phys. Lett. B **436** (1998) 55; Nucl. Phys. B **537** (1999) 47.
- [2] L. Randall and R. Sundrum, Phys. Rev. Lett. **83** (1999) 3370.
- [3] I. Antoniadis, Phys. Lett. B **246** (1990) 377; J.D. Lykken, Phys. Rev. D **54** (1996) 3693; P. Hořava and E. Witten, Nucl. Phys. B **460** (1996) 506; Nucl. Phys. B **475** (1996) 94.
- [4] K.R. Dienes, E. Dudas and T. Gherghetta, Nucl. Phys. B **557** (1999) 25.
- [5] N. Arkani-Hamed, S. Dimopoulos, G. Dvali and J. March-Russell, Phys. Rev. D **65** (2002) 024032.
- [6] A. Pilaftsis, Phys. Rev. D **60** (1999) 105023.
- [7] A. Ioannisian and A. Pilaftsis, Phys. Rev. D **62** (2000) 066001.
- [8] For example, see: G.R. Dvali and A.Y. Smirnov, Nucl. Phys. B **563**, 63 (1999); R.N. Mohapatra, S. Nandi and A. Perez-Lorenzana, Phys. Lett. B **466**, 115 (1999); A. Lukas, P. Ramond, A. Romanino and G.G. Ross, Phys. Lett. B **495**, 136 (2000); R. Barbieri, P. Creminelli and A. Strumia, Nucl. Phys. B **585**, 28 (2000); R.N. Mohapatra and A. Perez-Lorenzana, Nucl. Phys. B **593**, 451 (2001); A. Lukas, P. Ramond, A. Romanino and G.G. Ross, JHEP **0104**, 010 (2001); K.R. Dienes and I. Sarcevic, Phys. Lett. B **500**, 133 (2001); N. Cosme, J.-M. Frère, Y. Gouverneur, F.S. Ling, D. Monderen and V. Van Elewyck, Phys. Rev. D **63**, 113018 (2001); D.O. Caldwell, R.N. Mohapatra and S.J. Yellin, Phys. Rev. Lett. **87**, 041601 (2001); J. Maalampi, V. Sipilainen and I. Vilja, Phys. Lett. B **512**, 91 (2001); C. S. Lam and J. N. Ng, Phys. Rev. D **64**, 113006 (2001); A.S. Dighe and A.S. Joshipura, Phys. Rev. D **64**, 073012 (2001); A. Nicolaidis and D.T. Papadamou, Phys. Rev. D **66**, 013005 (2002); J.-M. Frère, M.V. Libanov and S.V. Troitsky, JHEP **0111**, 025 (2001); J.L. Hewett, P. Roy and S. Roy, Phys. Rev. D **70**, 051903 (2004); N. Arkani-Hamed and S. Dimopoulos, Phys. Rev. D **65**, 052003 (2002); T. Gherghetta, Phys. Rev. Lett. **92**, 161601 (2004).
- [9] G. Bhattacharyya, H.V. Klapdor-Kleingrothaus, H. Päs and A. Pilaftsis, Phys. Rev. D **67** (2003) 113001.
- [10] M. Fukugita and T. Yanagida, Phys. Lett. B **174** (1986) 45.
- [11] For example, see, E.G. Gimon and J. Polchinski, Phys. Rev. D **54** (1996) 1667.
- [12] Y. Grossman and M. Neubert, Phys. Lett. B **474** (2000) 361; G. Moreau, Eur. Phys. J. C **40** (2005) 539.
- [13] M. Cirelli, G. Marandella, A. Strumia and F. Vissani, Nucl. Phys. B **708** (2005) 215.
- [14] P. Aliani, V. Antonelli, M. Picariello and E. Torrente-Lujan, arXiv:hep-ph/0309156.
- [15] A. Bandyopadhyay, S. Choubey, S. Goswami, S.T. Petcov and D.P. Roy, Phys. Lett. B **583** (2004) 134.
- [16] For a review, see: A. Sirlin, talk delivered at the 1999 Lepton-Photon Conference, Stanford University, USA, August, 1999 Int. J. Mod. Phys. A **15** S1 (2000) 398.
- [17] See, *e.g.* N.F. Bell, FERMILAB-FN-0785-A, T.M. Ito and G. Prezeau, Phys. Rev. Lett. **94** (2005) 161802.
- [18] L. Covi, E. Roulet and F. Vissani, Phys. Lett. B **384** (1996) 16.
- [19] A. Pilaftsis and T.E.J. Underwood, Nucl. Phys. B **692** (2004) 303.
- [20] See, *e.g.* G.F. Giudice, A. Notari, M. Raidal, A. Riotto and A. Strumia, Nucl. Phys. B **685**, 89 (2004); W. Buchmüller, P. Di Bari and M. Plumacher, Annals Phys. **315** (2005) 305.
- [21] V.A. Rubakov and M.E. Shaposhnikov, Phys. Lett. B **125** (1983) 136.

- [22] N. Arkani-Hamed and M. Schmaltz, Phys. Rev. D **61** (2000) 033005; E.A. Mirabelli and M. Schmaltz, Phys. Rev. D **61** (2000) 113011; G. Dvali and M. Shifman, Phys. Lett. B **475** (2000) 295; G.C. Branco, A. de Gouvea and M.N. Rebelo, Phys. Lett. B **506** (2001) 115; M. Raidal and A. Strumia, Phys. Lett. B **553** (2003) 72.
- [23] H.V. Klapdor-Kleingrothaus and U. Sarkar, Phys. Lett. B **541** (2002) 332.
- [24] P. Minkowski, Phys. Lett. B **67** (1977) 421; M. Gell-Mann, P. Ramond and R. Slansky, *Proceedings of the Supergravity Stony Brook Workshop*, New York 1979, eds. P. Van Nieuwenhuizen and D. Freedman; T. Yanagida, *Proceedings of the Workshop on Unified Theories and Baryon Number in the Universe*, Tsukuba, Japan 1979, eds. A. Sawada and A. Sugamoto; R.N. Mohapatra, G. Senjanovic, Phys. Rev. Lett. **44** (1980) 912.